Implementation and Testing of Ice and Mud Source Functions in WAVEWATCH III®

W. Erick Rogers
Mark D. Orzech

Ocean Dynamics and Prediction Branch
Oceanography Division

April 19, 2013

REPORT DOCUMENTATION PAGE

Public reporting burden for this collection of information is estimated to average 1 hour per response, including the time for reviewing instructions, searching existing data sources, gathering and maintaining the data needed, and completing and reviewing this collection of information. Send comments regarding this burden estimate or any other aspect of this collection of information, including suggestions for reducing this burden to Department of Defense, Washington Headquarters Services, Directorate for Information Operations and Reports (0704-0188), 1215 Jefferson Davis Highway, Suite 1204, Arlington, VA 22202-4302. Respondents should be aware that notwithstanding any other provision of law, no person shall be subject to any penalty for failing to comply with a collection of information if it does not display a currently valid OMB control number. **PLEASE DO NOT RETURN YOUR FORM TO THE ABOVE ADDRESS.**

1. REPORT DATE (DD-MM-YYYY) 19-04-2013	2. REPORT TYPE Memorandum Report	3. DATES COVERED (From - To)

4. TITLE AND SUBTITLE

Implementation and Testing of Ice and Mud Source Functions in WAVEWATCH III®

5a. CONTRACT NUMBER

5b. GRANT NUMBER

5c. PROGRAM ELEMENT NUMBER
0601153N

6. AUTHOR(S)

W. Erick Rogers and Mark D. Orzech

5d. PROJECT NUMBER

5e. TASK NUMBER

5f. WORK UNIT NUMBER
73-4626-02-5

7. PERFORMING ORGANIZATION NAME(S) AND ADDRESS(ES)

Naval Research Laboratory
Oceanography Division
Stennis Space Center, MS 39529-5004

8. PERFORMING ORGANIZATION REPORT NUMBER

NRL/MR/7320--13-9462

9. SPONSORING / MONITORING AGENCY NAME(S) AND ADDRESS(ES)

Office of Naval Research
One Liberty Center
875 North Randolph Street, Suite 1425
Arlington, VA 22203-1995

10. SPONSOR / MONITOR'S ACRONYM(S)

ONR

11. SPONSOR / MONITOR'S REPORT NUMBER(S)

12. DISTRIBUTION / AVAILABILITY STATEMENT

Approved for public release; distribution is unlimited.

13. SUPPLEMENTARY NOTES

14. ABSTRACT

This report describes the implementation of two new physics routines in the phase-averaged model for wind-generated surface gravity waves, WAVEWATCH III. The first routine accounts for the attenuation of waves by sea ice. The second routine accounts for the attenuation of waves by a viscous fluid mud layer at the seafloor. No such routines existed previously in this model, though the model did previously represent the partial blocking/transmission of waves by sea ice via the model's propagation routines. Results from simple one-dimensional and two-dimensional tests are presented. Planned future improvements for the wave-ice physics package are given.

15. SUBJECT TERMS

WAVEWATCH III   Wave-ice interaction
Wave-mud interaction

16. SECURITY CLASSIFICATION OF:			17. LIMITATION OF ABSTRACT	18. NUMBER OF PAGES	19a. NAME OF RESPONSIBLE PERSON W. Erick Rogers
a. REPORT Unclassified Unlimited	**b. ABSTRACT** Unclassified Unlimited	**c. THIS PAGE** Unclassified Unlimited	Unclassified Unlimited	29	**19b. TELEPHONE NUMBER** (include area code) 228-688-4727

Standard Form 298 (Rev. 8-98)
Prescribed by ANSI Std. Z39.18

Contents

List of Figures

1 Introduction

This report documents progress in the implementation of two new types of source functions in the WAVEWATCH III® model. The WAVEWATCH model was originally developed at Delft University (Tolman 1991). In its current form, it is referred to as WAVEWATCH III® ("WW3"), developed at NOAA's NCEP (Tolman et al. 2002). At time of writing, the last public release of WW3 was WW3 version 3.14 (Tolman 2009), and WW3 version 4 is under active development via a Subversion (svn) software versioning and revision control system administered by NCEP.

The governing equation of WW3 and most other "third generation" or "3G" wave models is the action balance equation. Simplified here from the WW3 form for purposes of presentation, the action balance equation is:

$$\frac{\partial N}{\partial t} + \frac{\partial C_x N}{\partial x} + \frac{\partial C_y N}{\partial y} + \frac{\partial C_\sigma N}{\partial \sigma} + \frac{\partial C_\theta N}{\partial \theta} = \frac{S}{\sigma} \tag{1}$$

The prognostic variable is the wave action density N, equal to energy density divided by angular relative frequency ($N = E/\sigma$), and is a function of space and time, $N = N(x, y, \theta, \sigma, t)$. Relative frequency σ is the wave frequency measured from a frame of reference moving with a current, if a current exists; θ is wave direction; C is the wave action propagation speed in $(x, y, \theta, \sigma, t)$ space. In absence of currents, C_x is the x-component of the group velocity C_g. The right hand side of the governing equation is the total of source/sink terms expressed as rate of change of wave action density, where $S = S(x, y, \theta, \sigma, t)$ is most generally represented by three terms, $= S_{in} + S_{nl} + S_{ds}$: input by wind, nonlinear interactions, and dissipation, respectively.

Sea ice and mud affect the length and dissipation rate of wind-generated ocean waves. The ice-modified (or mud-modified) wavenumber can be expressed as a complex number $k = k_r + ik_i$, with the real part k_r representing impact of the sea ice/mud on the physical wavelength and propagation speeds, producing something analogous to shoaling and refraction by bathymetry, whereas the imaginary part of the complex wavenumber, k_i, is an exponential decay coefficient $k_i(x, y, t, \sigma)$ (depending on location, time and frequency, respectively), representing wave attenuation, and can be introduced in a wave model such as WW3 as $S_{ice}/E = -2C_g k_i$, where S_{ice} is one of several dissipation mechanisms, along with whitecapping, for example, $S_{ds} = S_{wc} + S_{ice} + S_{mud} + \cdots$ on the right-hand side of the governing equation (see also Komen et al. (1994, pg. 170)). The k_r modified by ice/mud would enter the model via the C calculations on the left-hand side of the governing equation. Though the procedure is non-trivial with regard to necessary code changes, especially with regard to i/o, the fundamentals are straightforward, e.g. Rogers and Holland (2009 and subsequent unpublished work) modified a similar model, SWAN (Booij et al. 1999) to include the effects of a viscous mud layer using the same approach ($k = k_r + ik_i$) previously. The wave-*mud* interaction theory implemented by Rogers and Holland (2009) was derived by Ng (2000) for a viscous mud layer under a (very weakly) viscous water layer. This "two layer" approach is taken in some solutions for wave-*ice* interaction theory, e.g. Keller (1998), though he assumes that the water layer is inviscid, and of course the second layer is above rather than below the water layer.

In this report, we describe the implementation of new routines to represent the effect of ice and mud on waves in the WAVEWATCH III model. Both implementations utilize the concept of complex wavenumber $k = k_r + ik_i$. However, only the imaginary component is addressed in WW3 in this report (thus it is more limited than what was done for mud in the SWAN model). Modification of the real part has, at time of writing, not been addressed yet in WW3, though this is part of our plans.

General code modifications are described in Section 2. Rather than provide further background information for the two source terms here, we introduce them in their respective sections. Section 3 deals with the effect of ice on waves. Section 4 deals with the effect of mud on waves. Suggestions for further work are discussed in Section 5.

2   WW3 code: input methods

With regard to model coding, the most challenging task associated with this project so far has been not in the source term routines themselves, but rather in the code associated with the processing of user input. The latter is necessary since the new source terms require new variables to be input by the user. In the case of mud, we introduce new variables: mud thickness, mud viscosity, and mud density. In the case of ice, we allow up to five new parameters. These can be referred to generically as $C_{ice,1}$, $C_{ice,2}$, …, $C_{ice,5}$. In the code, $C_{ice,1}$ is referred to as "ICECOEF1" (a local scalar parameter in the source function routine) or "ICEP1" (a 2D array shared to the source function routine via a module which describes the spatial variation of the parameter on the computational grid). Our intent here is to allow the meaning of the ice parameters to vary depending on which S_{ice} routine is selected. For example, in an implemented S_{ice} routine (described below, referred to as the "Liu routine"), $C_{ice,1}$ represents the ice thickness (in meters) and $C_{ice,2}$ represents the eddy viscosity in the turbulent boundary layer beneath the ice.

Some remarks about this strategy:

1) External variables already available, like currents, water depth, wind, ice concentration can also be used (though probably only ice concentration is useful for S_{ice}) and do *not* count against the maximum total of 5 parameters.

2) External variables not already available, like water temperature, salinity, ice thickness, effective viscosity, could be used but *would* count against the maximum total of 5 parameters.

3) If a developer feels that the five ice parameters and three mud parameters are insufficient, these numbers can be increased, but unfortunately, this is not easy to code. We point out that since these are rather specific and specialized physics routines, there probably will not be many situations in which ice and mud are used in the same simulation. A developer can potentially exploit this by using mud "parameter space" for ice, as $C_{ice,6}$, $C_{ice,7}$, $C_{ice,8}$.

4) Ideas for potential use of the ice parameters are discussed in Section 5.

The new parameters are read in using the same methods that already exist for other scalar parameters, such as ice concentration and water level. The variables are allowed to vary in time and space. In case of spatially varying parameters, these are read in via the ww3_prep program,

using instructions in the ww3_prep.inp user-input file. Otherwise, the user can use the simpler option of specifying them as homogeneous (but potentially time-varying) fields via the ww3_shel program, using instructions in the ww3_shel.inp user-input file. Though the latter method is simpler, it is not expected to find much use other than for idealized test cases. The ww3_prep approach of WW3 supports a number of different methods of user input. For example, the user can provide the ice parameters as ascii files on a non-WW3 grid, and ww3_prep will interpolate in time and space to the WW3 computational grid(s).

The WW3 code and test cases described in this report are kept on the NRL svn repository, which was last synchronized with the trunk of the NCEP svn repository at revision 21198 (Sep. 19 2012). The latest revision to the NRL svn repository at time of writing was 228.

3 Effect of ice on waves

The implementation of S_{ice} is described in this section.

3.1 Background: wave modeling in the Arctic

The mutual interactions between ocean waves and sea ice cover play a crucial role for planning safe operations in the Arctic Ocean. Therefore, wave and ice interactions should be among the center-pieces of the operational wave forecasting system. A research objective of NRL and the Office of Naval Research (ONR) is to study these interactions in the marginal ice zone (MIZ) of the Arctic Ocean, and develop techniques for modeling the effect of sea ice on wave energy and wavelength. A number of theories and models have been developed to describe this phenomenon, e.g. Keller (1998), Liu et al. (1991), Squire et al. (1995), Wadhams et al. (1986), Wadhams et al. (1988), and Wang and Shen (2010). A brief review of these methods is given in the Appendix (Section 8).

The retreating ice cover implies an increase in fetch for generation of waves in the Arctic. This, combined with more frequent incoming cyclones in the Arctic (Sepp and Jaagus 2011) naturally leads to more severe wave conditions. The reduction of the permanent polar pack ice also implies that regions of the Arctic that could previously be ignored in operational numerical wave models must now be considered. Fortunately, NRL has recently extended the capability of the WAVEWATCH III (WW3, Tolman 1991, 2009) model so that it can be applied on irregular grids (Rogers and Campbell 2009). An implementation of WW3 for the Arctic has been successfully demonstrated in the beta queue at FNMOC (Fleet Numerical Meteorology and Oceanography Center), on the same grid as used for the Arctic atmospheric model (COAMPS, Hodur 1997), with significantly better resolution (15-20 km)—and better forcing—than that of the global wave model. Figure 1 and Figure 2 below shows examples of test simulations on this grid. During FY11, NRL has extended WW3 to allow use of two-way nesting "mosaic" approach of Tolman (2008) with curvilinear grids. Realtime surface current and ice concentration values are available from the 1/12° Arctic Cap Nowcast/Forecast System (ACNFS), developed at NRL (Posey et al. 2010). Further, within the next two years, funded by the Earth System Prediction Capability (ESPC) program, NRL will begin transitioning to the Naval Oceanographic Office (NAVOCEANO) an Earth System Model Framework (ESMF)-based, coupled wave-ocean model on a global high resolution tripolar grid. Both wave model grid methods, the curvilinear two-way nested Arctic regional grid and the global tripolar (curvilinear) grid, address the traditional problems associated with extending a regular global grid to high latitudes, e.g. the

operational WW3 at FNMOC stops at 78° latitude. With all this in mind, we can see that from a technical standpoint, the operational Navy is well-positioned for forecasting waves in the Arctic over the next decade.

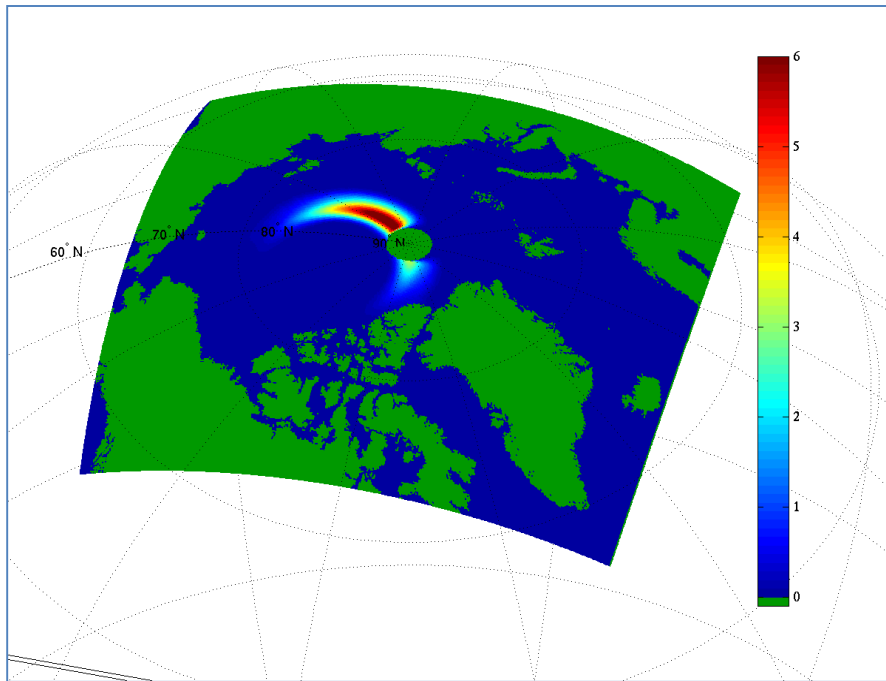Figure 1. Propagation test with WAVEWATCH III model on curvilinear Arctic grid. [Significant waveheight H_s in meters] No ice, winds, or boundary forcing are included, and the region above 89° is treated as land to avoid directional singularity. The initial condition (geographic distribution) is a Gaussian spike in the wave field. The plotted condition is after several hours of propagation.
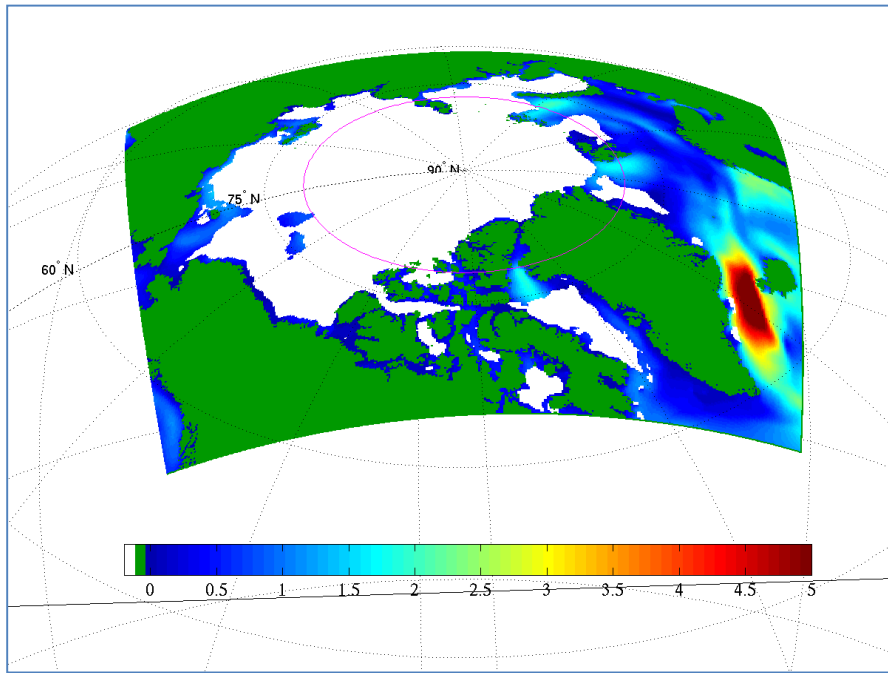
4

Figure 2. Source term test with WAVEWATCH III model with global and Arctic grid. The curvilinear Arctic grid is shown here. [Significant waveheight H_s in meters] Ice, winds, and boundary forcing are included in this hindcast. This is the result at May 25 2009 12Z, after a 12 hour simulation (from cold start). In this simulation, two-way nesting is performed, such that wave spectra from this nest can propagate across the boundary into the global model, and vice versa.

Unfortunately, the situation with regard to the physics of wave models in the Arctic is much less optimistic. The key physical process, wave attenuation by interaction with ice floes in the Marginal Ice Zone (MIZ), is treated within the propagation routine of the model, with the percent transmission of wave energy through ice being a simple function of ice concentration. There is no connection to any physical mechanism for wave attenuation; this artificial "dissipation" is not dependent on frequency and has a spurious dependence on grid aspect ratio (Section 3.2). This simple, non-physical approach could nevertheless be justified on the grounds that operational characterization of the ice is limited (ice concentration only) and further that the existing physical mechanisms available from the literature which might be implemented in the forecast model are 1) too numerous and too varied to select from and 2) too poorly informed, e.g. what is the value of a theoretical model which requires input parameters that are impossible to estimate? Compounding the problem is a very limited number of studies estimating attenuation from observations, which would normally be used to calibrate and verify a numerical model.

As mentioned above, a specific NRL research objective is to develop techniques for modeling the effect of sea ice on waves. In the present effort, we utilize modeling codes that are currently used operationally—WW3 in the case of the wave model—distinguishing our aim from more detailed process-based modeling investigations, such as models of individual waves and ice floes.

5

3.2 Background: existing methods vs. new methods of representing the effect of ice on waves

The existing method of treating ice is described by Tolman (2003, 2009). Ice concentration $\epsilon(x, y, t)$ is specified by the user, in addition to two constant parameters which describes the minimum concentration which affects the waves, $\epsilon_{c,0}$ and the concentration at which wave energy is completely blocked, $\epsilon_{c,n}$. For example, the parameters might be set at $\epsilon_{c,0} = 0.25$ and $\epsilon_{c,n}$=0.75. For ice concentrations between $\epsilon_{c,0}$ and $\epsilon_{c,n}$, the wave energy is partially blocked/transmitted based on linear interpolation between the two values: the cell transparency in the x direction is calculated as $\alpha_x(x, y, t) = (\epsilon_{c,n} - \epsilon(x, y, t))/(\epsilon_{c,n} - \epsilon_{c,0})$. This method necessitates grid-specific calibrations; this characteristic is perhaps best illustrated by recognizing that as $\Delta x \to 0$, the method will give infinite dissipation.

In the v3.14 public release of WW3 (Tolman 2009), the amount of blocking had an unfortunate additional dependence on grid aspect ratio, but this was removed in the development version (v4), by Dr. Ardhuin (Ifremer). A contemporary change was to add an option to replace this α_x calculation with a new one: $\alpha_x(x, y, t) = \exp(-\epsilon(x, y, t)\Delta x)/L_\epsilon$, where L_ϵ (denoted "FICEL" and "LICE" in the code) is a new user-specified constant parameter, apparently a dissipation length scale. It can be shown that for ϵ=1 and $L_\epsilon = 1/k_i$ this method is a numerical approximation of the analytical formula given by (5) below. This further implies that the method is effectively similar to our first method described in Section 3.3.1, but using variable ice concentration $\epsilon(x, y, t)$ and the additional constant parameter L_ϵ in place of the variable parameter $k_i(x, y, t)$. The original parameters $\epsilon_{c,0}$ and $\epsilon_{c,n}$, are not used by this new, optional method. This method is not documented.

In any case, these existing methods represent the dissipation of waves by interaction with sea ice using the LHS of (1) (propagation/blocking), and our objective here is to move this to the RHS of (1) (dynamics).

Reflection by icebergs (distinct from sea ice) is added to the development version of the code by Dr. F. Ardhuin. This new feature is documented in the development version of the manual. This is added primarily to address the overprediction of significant waveheight (SWH) by global operational models near Antarctica.

3.3 WW3 code: method of including S_{ice}

The methods of user-input has already been explained above. In this section, we describe two methods of calculating S_{ice} which we have implemented in WW3. It is anticipated that additional methods, e.g. Keller (1998), Wang and Shen (2010), will be implemented in the future.

In comparison to the Tolman (2003) method of representing the dissipation by ice as a per-cell partial blocking mechanism on the LHS of equation (1), the new method is to treat as a source term on the RHS of equation (1). The new method has the advantage of removing the proportional dependence of dissipation on resolution. As $\Delta x \to 0$, the old method would give infinite dissipation, whereas the new method converges to a proper, continuous solution.

<u>Technical details</u>. To follow the WW3 convention, each S_{ice} method would have a Fortran file associated with it. However, to simplify code during the development process, the two S_{ice} methods are kept in the same Fortran file (w3sic1md.ftn) for now, and the user selects the S_{ice} method using a namelist variable. At a later stage, these will be expanded into multiple Fortran files (w3sic1md.ftn, w3sic2md.ftn w3sic3md.ftn, etc.) which are selected via "switch"

file, following WW3 convention. Though the latter approach unfortunately tends to result in substantial repeated/redundant code, it is highly beneficial when multiple groups develop source term methods.

3.3.1 Method 1: dissipation rate constant in frequency space.

The first implemented method is for the user to specify $k_i(x, y, t)$ which is uniform in frequency space, $C_{ice,1} = k_i$. In this case, the amount of information read in has not changed from the Tolman (2003) method of using ice concentration, $\epsilon(x, y, t)$.

3.3.2 Method 2: Liu et al. (1991)

This method is based on the papers by Liu and Mollo-Christensen (1988) and Liu et al. (1991); these will be denoted as "LMC" and "LHV" here. This is a model for "viscous attenuation by a sea ice cover", derived on the assumption that dissipation is caused by turbulence in the boundary layer between the ice floes and the water layer, with the ice modeled as a continuous thin elastic plate. As mentioned above, input ice parameters are ice thickness (in meters) and an "eddy viscosity in the turbulent boundary layer beneath the ice", ν. $C_{ice,1}$ represents the former and $C_{ice,2}$ represents the latter. Ice concentration is *not* an input to this routine; this is discussed further below.

A description of the code follows:
1. <u>General routine</u>. If non-zero $C_{ice,1}$, the forward dispersion routine (item 2 below) is called. This is used to calculate α, the spatial exponential decay rate of energy[1]. From there, $D = -2C_g k_i$, and finally $S_{ice} = DN$. Here, D represents the temporal decay rate, $D = S_{ice}/E$. Recall from above that C_g is group velocity, S is the source term (following WAMDI (1988) convention), E is spectral energy density and $N = E/\sigma$ is spectral action density. The variable D varies in frequency space but is constant in directional space. The variable S_{ice} varies in directional space via dependence on N. Further, recall that C_{ice} parameters vary in geographic space and time, e.g. $C_{ice,1}(x, y, t)$.
2. <u>Forward dispersion relation routine</u>. This is very much like a traditional dispersion relation: given frequency f, find wavenumber k. However, in this case, the wavenumber is a complex number. The LHV dispersion relation cannot be solved directly, so Newton-Raphson method is used here, calling the "reverse dispersion" routine (item 3 below), which is directly solvable. Inputs to this routine are (all being local terms): ice thickness, eddy viscosity, water depth, and f. Output from this routine are: k_r, C_g, α. The first two can potentially be used later to feed back to model kinematics, to produce refraction (in case of k_r) and shoaling (in case of C_g) by ice. Only α is relevant to the S_{ice} calculation.
3. <u>Reverse dispersion routine</u>. This is a directly solvable calculation using the equations of LHV. Inputs to this routine are: ice thickness, eddy viscosity, water depth, k_r. Outputs from this routine are: f, C_g, and α.

<u>Equations</u>:
The reader is referred to LHV, equations on page 4606. The key equations are:

---

[1] Note: α is exponential decay rate of energy while k_i is exponential decay rate of amplitude, so $k_i = \alpha/2$. There is no intended connection between α and α_x, the latter being the variable used by Tolman (2009) to represent cell transparency.

$$\sigma^2 = (gk_r + Bk_r^5)/(\coth(k_rh_w) + k_rM) \tag{2}$$

$$C_g = (g + (5 + 4k_rM)Bk_r^4)/(2\sigma(1 + k_rM)^2) \tag{3}$$

$$\alpha = \left(\sqrt{\nu\sigma}k_r\right)/\left(C_g\sqrt{2}(1 + k_rM)\right) \tag{4}$$

In our notation, h_w is water depth and h_i is ice thickness. There is an apparent typo in equation (1) of LHV, coth (kh_i) should be coth (kh_w). The variables B and M quantify the effects of the bending of the ice and inertia of the ice, respectively. Both of these variables depend on h_i (for these equations, see LMC).

Example calculations of dissipation rate α using the LHV model are shown in Figure 3. In this case, the three described routines are coded in Matlab, but they have been re-coded in Fortran for the purpose of application in WW3.
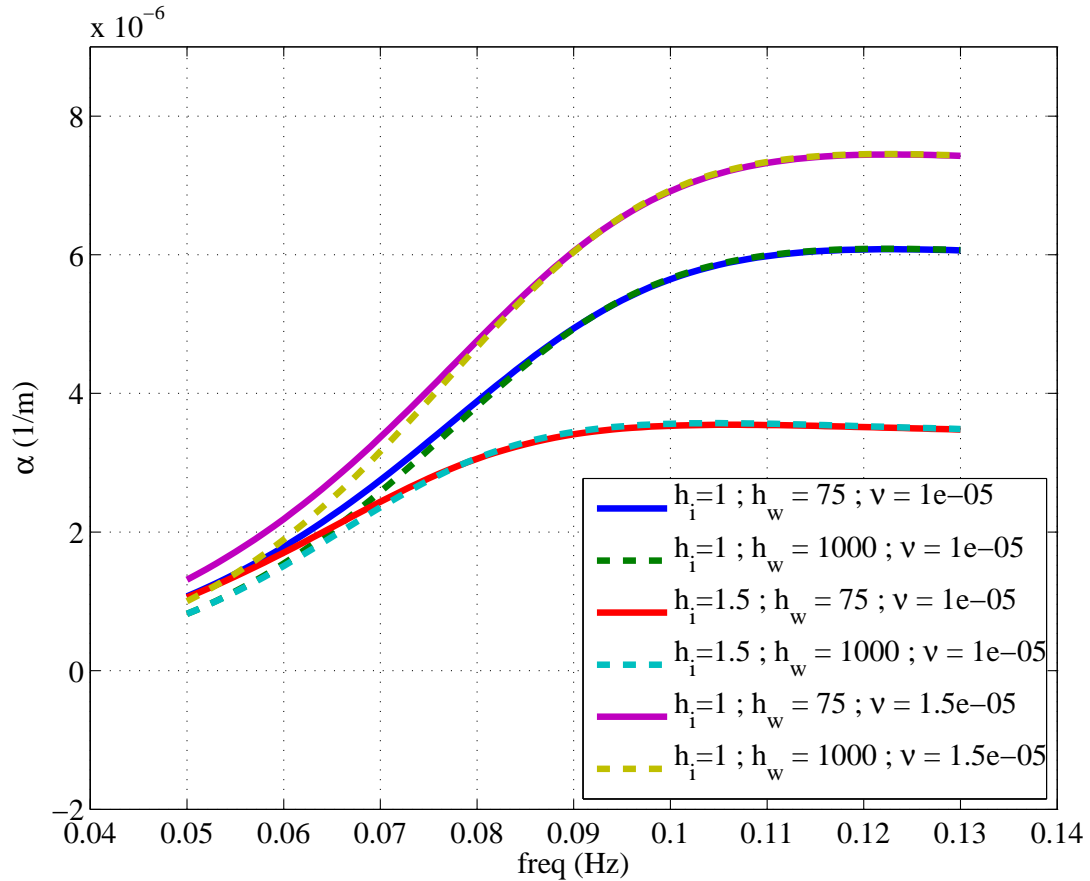

Figure 3. Example calculations of dissipation rate α using the LHV model, coded using the three routines as described in the text. Units of h_w and h_i are in meters; units of ν are m^2/sec.

8

LHV state: "The only tuning parameter is the turbulent eddy viscosity, and it is a function of the flow conditions in the turbulent boundary layer which are determined by the ice thickness, floe sizes, ice concentration, and wavelength." The eddy viscosity term ν given by LHV is unfortunately "highly variable" (their words), and "not a physical parameter", which suggests that it is difficult to specify in practice. In LHV, many values are referenced and used[2]:

1. ν=160.0× 10^{-4} m^2/sec (Brennecke 1921)
2. ν=24.0× 10^{-4} m^2/sec (Hunkins 1966)
3. ν=3450.0× 10^{-4} m^2/sec (LHV Fig. 11)
4. ν=4.0× 10^{-4} m^2/sec (LHV Fig. 12)
5. ν=150.0× 10^{-4} m^2/sec (LHV Fig. 13)
6. ν=54.0× 10^{-4} m^2/sec (LHV Fig. 14)
7. ν=384.0× 10^{-4} m^2/sec (LHV Fig. 15)
8. ν=1536.0× 10^{-4} m^2/sec (LHV Fig. 16)

Another criticism of this source term is that it does not use the ice concentration in actual calculations. The model assumes a continuous ice layer (100% concentration), so the method appears to simply rely on concentration being high: "When the ice is highly compact with high concentration, the flexural waves obey the dispersion relation…as similar waves in a continuous ice sheet." Later, "Five of these cases with high ice concentration (larger than 60%) in the MIZ have been selected". For general use, it would be better to include concentration in the calculations. This might be added by incorporating concentration as a scaling factor.

Other settings; all three are from LHV, pg. 4606 are:
1) Young's modulus of elasticity is set to $E = 6.0 \times 10^9$ N/m^2
2) Poisson's ratio is set to $s = 0.3$.
3) The relation between ice density and water density: $\rho_i = 0.9\rho_w$.

3.4   One-dimensional tests with S_{ice}

Figure 4 shows results for a simple one-dimensional test case. The analytical expression used here is:

$$H(x) = H_0 e^{-k_i x} \tag{5}$$

where H is significant waveheight and H_0 is significant waveheight at $x = 0$. In Figure 4, $\Delta x = 1$ km is used. The model captures the decay well for weaker dissipation values, but at the highest dissipation values, the model decay is somewhat slower than the analytical solution. Even with the highest dissipation rate, the error might be considered tolerable. To demonstrate sensitivity to geographic resolution, results with $\Delta x = 10$ km are shown in Figure 5. In this case, the numerical error for the higher dissipation rates is clearly not acceptable. These results suggest that expected dissipation rates must be part of the decision with respect to what resolution to use: if k_i is large, then the spatial resolution cannot be too coarse, or the numerical representation is poor.

---

[2] Note: In our implementation, the user specifies eddy viscosity in units of m^2/sec even though values are given in units of cm^2/sec in LHV.
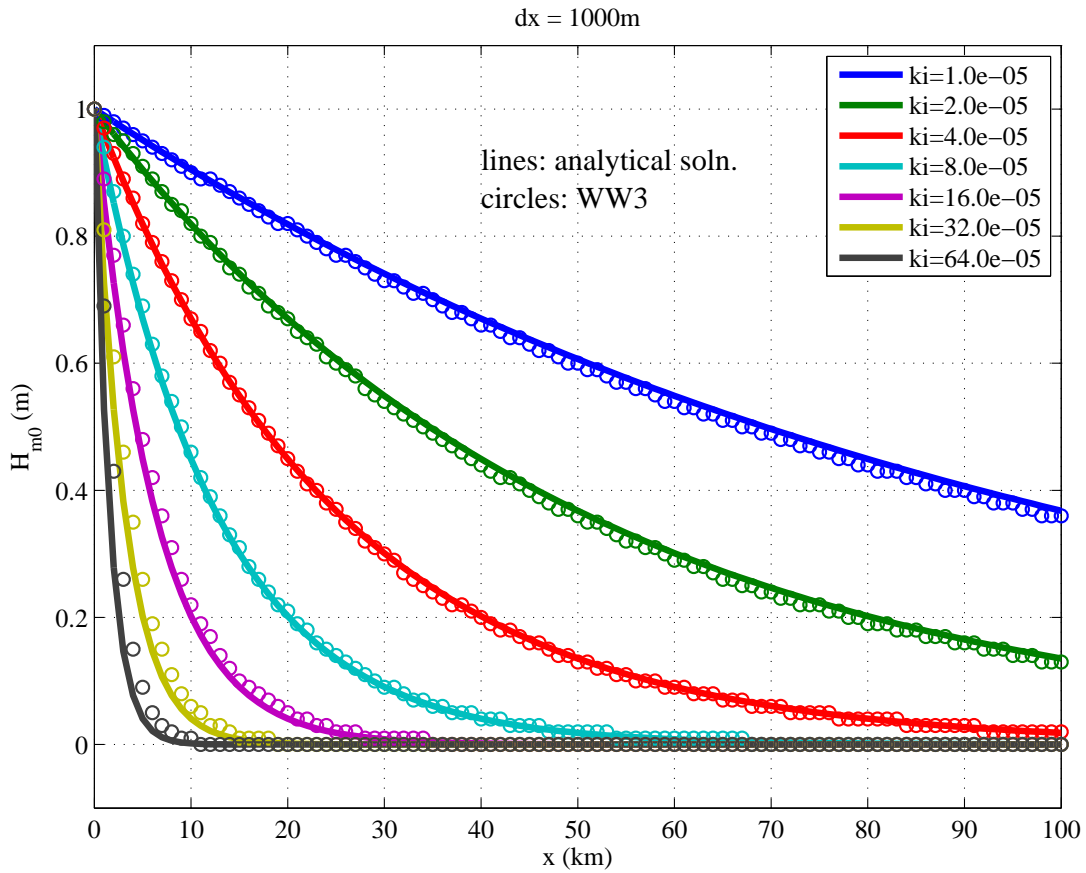
Figure 4. One-dimensional tests using $\Delta x = 1$ km. Significant waveheight is plotted. Waves are initialized at the left boundary, $x = 0$. Results using various k_i settings are shown. Units of k_i are 1/m. The dissipation rate k_i is stationary and constant in x and in frequency space. Solid lines: calculations using an analytical expression. Circles: WW3 output. This test case is included in the NRL svn repository for WW3.
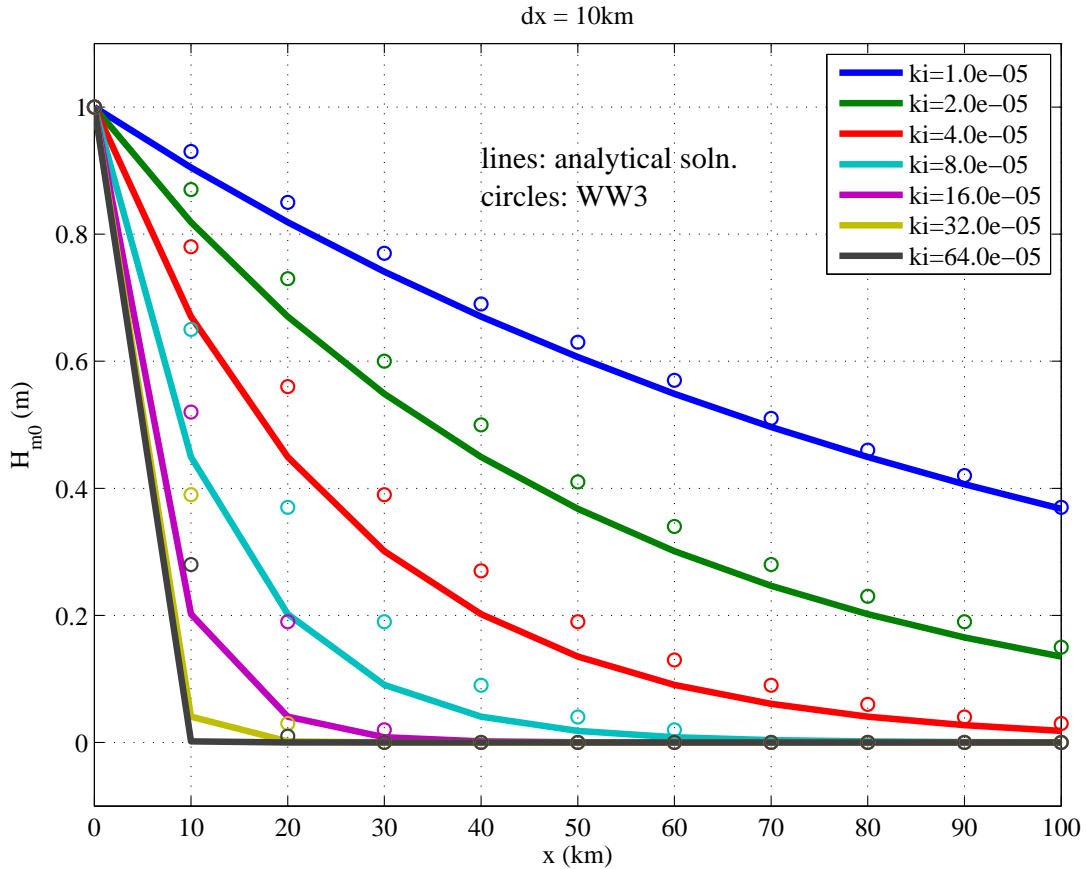
Figure 5. Identical to Figure 4, except that $\Delta x = 10$ km is used.

The question of "how much error is tolerable" is, of course, subjective. If we assume that 2.7% error in H_{m0} is intolerable in our idealized simulations, experiments with a number of resolutions can be summarized as follows (with k_i given in m^{-1}).

- for Δx=20.0 km, k_i should not exceed 3.5e-6
- for Δx=5.0 km, k_i should not exceed 2.0e-5
- for Δx=2.5 km, k_i should not exceed 5.0e-5
- for Δx=1.0 km, k_i should not exceed 2.0e-4 (assumes 2.7% Hs error is intolerable)
- for Δx=0.35 km, error is less than 2.1% for all k_i tested (up to 1.0e-3)
- for Δx=0.10 km, error is less than 1.3% for all k_i tested (up to 1.0e-3)

For reference, Arctic Cap Nowcast/Forecast System (Posey et al. 2010) is 1/12°, so Δx=9.25 km north-south.

The analytical formula also allows us to put the dissipation rate of the original model (partial blocking due to ice concentration) in context with k_i values. For example, if the original model has a grid cell with 50% blocking, and has resolution of 55 km, this is equivalent to $k_i = 1.26 \times 10^{-5}$ m^{-1}.

11

3.5 Two-dimensional tests with S_{ice}

Two two-dimensional test cases have been added to the svn repository for WW3. The first, like the one-dimensional test case of the previous section, uses a k_i value read in from input files which is constant in frequency space. The domain is square, with $n_x = n_y = 51$ and $\Delta x = \Delta y = 5$ km. Boundary forcing is uniform and steady along the southern and eastern boundaries, producing swells propagating from the southeast ($\theta = 135°$). The initial condition is a uniform wave field equivalent to the boundary forcing. In the northwest quadrant of the domain, ice appears and disappears during the duration, with $k_i = 0$, $k_i = 1 \times 10^{-5}$ m^{-1}, $k_i = 2 \times 10^{-5}$ m^{-1}, $k_i = 1 \times 10^{-5}$ m^{-1}, and then $k_i = 0$. Results from this test case are not shown, but are consistent with expectations: the non-stationary, non-uniform ice specification is validated to work as intended.

The second two-dimensional test case uses the Liu et al. (1991) attenuation model, with ice thickness of 1 m and ice eddy viscosity parameter $v_e = 1 \times 10^{-4}$ m^2/sec. The computational grid uses three frequencies: 0.08 Hz, 0.10 Hz, and 1.25 Hz, with most of the energy in the specified boundary forcing corresponding to the central frequency. With this model, k_i is, of course, frequency-dependent. For these three frequencies and ice parameters, $k_i = 6.0 \times 10^{-6}$, 8.9×10^{-6}, and 9.5×10^{-6} m^{-1} respectively. The computational grid is square, with $n_x = 101$, $n_y = 51$, $\Delta x = 5$ km, and $\Delta y = 10$ km. As in the other two-dimensional test, the boundary forcing is uniform and steady along the southern and eastern boundaries, producing swells propagating from the southeast ($\theta = 135°$). The initial condition consists of near-zero wave energy on the interior of the domain. Ice is again specified in the northwest quadrant, but unlike the other two-dimensional test, in this test, ice conditions are stationary. Swell propagates into the ice and eventually a steady state is reached, with total simulation duration being 30 hours. The final state is shown in Figure 6.
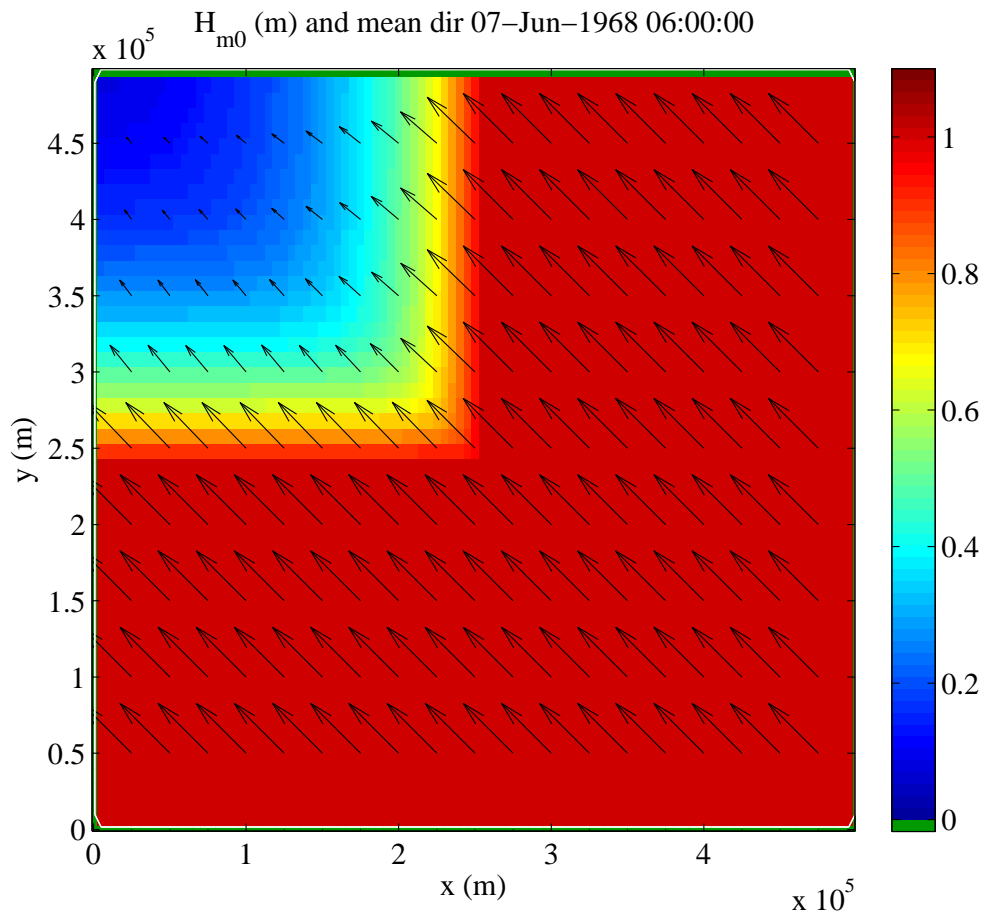
Figure 6. Final state of the second two-dimensional test case, as explained in the text.

4 Effect of mud on waves

Wave damping by muddy seabeds is generally understood to occur when wave-generated stresses exceed the limiting strength of the bed, causing the liquefaction of some or all of the mud layer into a viscous "fluid mud". Internal waves are then generated at the water-mud interface, and their energy is dissipated relatively rapidly by viscosity within the fluid mud layer. Several theoretical approaches have been used to model the effect of mud on waves, representing the mud as a purely viscous fluid (e.g., Dalrymple and Liu, 1978; Ng, 2000; Winterwerp et al., 2007), or alternatively as viscoelastic (e.g., MacPherson, 1980; Jiang and Mehta, 1996; Zhang and Ng, 2006) or plastic (e.g., Mei and Liu, 1987).

Until recently, the effect of mud on waves has had little or no representation in generally available nearshore wave models such as SWAN (Booij et al., 1999) and WW3, which have been limited to rigid beds. This has been a major shortcoming, forcing users to specify unrealistic bottom friction parameters in muddy areas in order to get the desired wave dissipation characteristics.

The present section describes the implementation in WW3 of two viscous fluid mud dissipation formulations, borrowing heavily from very similar implementations added to the SWAN wave model by Rogers and Holland (2009).

13

4.1   Background: implementation in SWAN

Three formulations for wave damping by purely viscous mud have been implemented in SWAN. The first formulation (Rogers and Holland, 2009, based on Dalrymple and Liu, 1978) treats the mud as a laminar viscous fluid. This is a relatively accurate method, but it requires a complex iterative technique which significantly lengthens computational time. The second formulation (Rogers and Holland, 2009, based on Ng, 2000) is simplified relative to Dalrymple and Liu (1978) in that it assumes the mud layer to be thin. This formulation computes a mud-induced group velocity from the real part of the mud-induced wavenumber, which allows the effects of mud on wave refraction, shoaling, and de-shoaling to be estimated. The third formulation (Winterwerp et al., 2007) integrates the energy transport across the water/mud interface over one wave period, based on earlier work by Gade (1958) and De Wit (1995). Unlike the other implementations, it assumes the water to be inviscid and does not consider mud effects on wave phase and group velocities.

4.2   WW3 code: method of including S_{mud}

For the present project, two of the above formulations for the dissipation of wave energy by viscous mud were implemented in WW3. The first implementation (module "w3sbt8md") is based on the formulation of Dalrymple and Liu (1978). A second implementation (module "w3sbt9md") is based on the formulation of Ng (2000). The code that was originally created for these formulations in the spectral wave model SWAN was transferred, with a small number of modifications, directly into the WW3 modules. Additional modifications were made to several other WW3 subroutines to allow users to turn on/off the mud dissipation routines and to input field data for mud thickness, density, and kinematic viscosity (Section 2).

A description of the WW3 code follows:

1.   General routines. If the user specifies "BT8" or "BT9" in the "switch" parameter file, the preprocessor will activate code statements calling the w3sbt8 or w3sbt9 subroutines in the computation of source terms by module w3srcemd. For non-uniform input fields, the user must create "ww3_prep" input files for each of the mud-related parameters: mudd (density), mudt (thickness), and mudv (viscosity). Field data on the distribution of mud parameter values throughout the grid are read either from these files or from separate field parameter files referenced in the prep files.

2.   Dalrymple & Liu routine (w3sbt8). The wave dissipation by the fluid mud is computed using an iterative procedure that converges to the complex mud-induced wave number, k_{mud}. Dissipation due to mud at each frequency is determined from the imaginary part of this wave number as

$$D_{mud} = 2 \cdot imag(k_{mud}) \cdot C_{g,mud} \qquad (6)$$

where $C_{g,mud}$ is the mud-induced wave group velocity. This dissipation is added to contributions from other source/sink terms by w3srce. For additional details, see Dalrymple & Liu (1978).

14

3. <u>Ng routine (w3sbt9)</u>. After initialization of mud field data and assignment/computation of various local parameters, the w3sbt9 routine calls the "Ng" subroutine to compute the mud-induced dissipation. The Ng routine determines two second-order coefficients $(B_r^{'}, B_I^{'})$ that are then used to compute wave attenuation due to mud as follows:

$$D_{mud} \equiv imag(k_2) = -\frac{\delta_m\left(B_r^{'} + B_I^{'}\right)k_1^2}{\sinh 2k_1 h + 2k_1 h} \qquad (7)$$

where δ_m is the Stokes boundary layer thickness for mud, h is water depth, and k_1 and k_2 are the first- and second-order parts of the wave number, respectively, in a Taylor expansion about the mud-water interface. For additional details, see Ng (2000). Results from the Ng subroutine are returned to w3sbt9, which passes them back to w3srce where the mud-induced dissipation is again added to contributions from other source/sink terms.

Note a fixed value for water kinematic viscosity "nu_water" (1.31E-6 m^2/s) was added to the module "constants" (i.e., file "constants.ftn"). This is the kinematic viscosity of pure water at 10°C and is in accordance with the water density value (1000 kg/m^3) that is used throughout WW3. This value for kinematic viscosity of water is used in both w3sbt8 and w3sbt9.

4.3   One-dimensional test cases with S_{mud}

Test cases ("mud_test1" and "mud_test2", respectively) were created for WW3 to simulate 1D wave propagation for a distance of 100 km over a flat bottom with a mud layer of constant thickness using each of the above formulations. Parameters for both tests are generally set to match those used in Fig. 3 of Rogers and Holland (2009), except for mud thickness and grid size/spacing. These quantities are allowed to vary in order to investigate their effects on model accuracy.

The following is a list of features of both 1D test cases:

- spectral, spatial, and time settings:
  - three (3) frequencies from 0.08 to 0.125 Hz; 24 directions
  - initial wave height = 1.0 m
  - nx=24–120, ny=3
  - Δx=Δy=1.0 to 5.0 km
  - boundary forcing from west boundary
  - boundary forcing: θ=270° (waves from southeast), f_p=0.10 Hz
  - Starting time : 1968/06/06 00:00:00 UTC
  - Ending time   : 1968/06/06 12:00:00 UTC
- mud parameters are constant for entire domain:
  - mud density=1310 kg/m^3
  - mud thickness=0.01 - 0.4 m
  - mud viscosity=7.60E-03 m^2/s

The objective of these tests is to compare the actual decay calculated by WW3 with the methods of Dalrymple and Liu (1978) and Ng (2000) to the expected exponential decay. For the comparison, multiple values were used for mud thickness, which caused the the exponential

15

decay coefficient, k_i, to range from 0.23e-05 to 12.74e-05 m^{-1}. As seen earlier with ice dissipation, model accuracy was affected by the grid spacing used in these calculations. Figure 8 shows estimated H_{m0} values (circles and asterisks) plotted versus theory (i.e., Eq. 5; solid lines) for grid spacing of Δx = 1 km, while Figure 8 shows the same comparisons for grid spacing of Δx = 5 km.
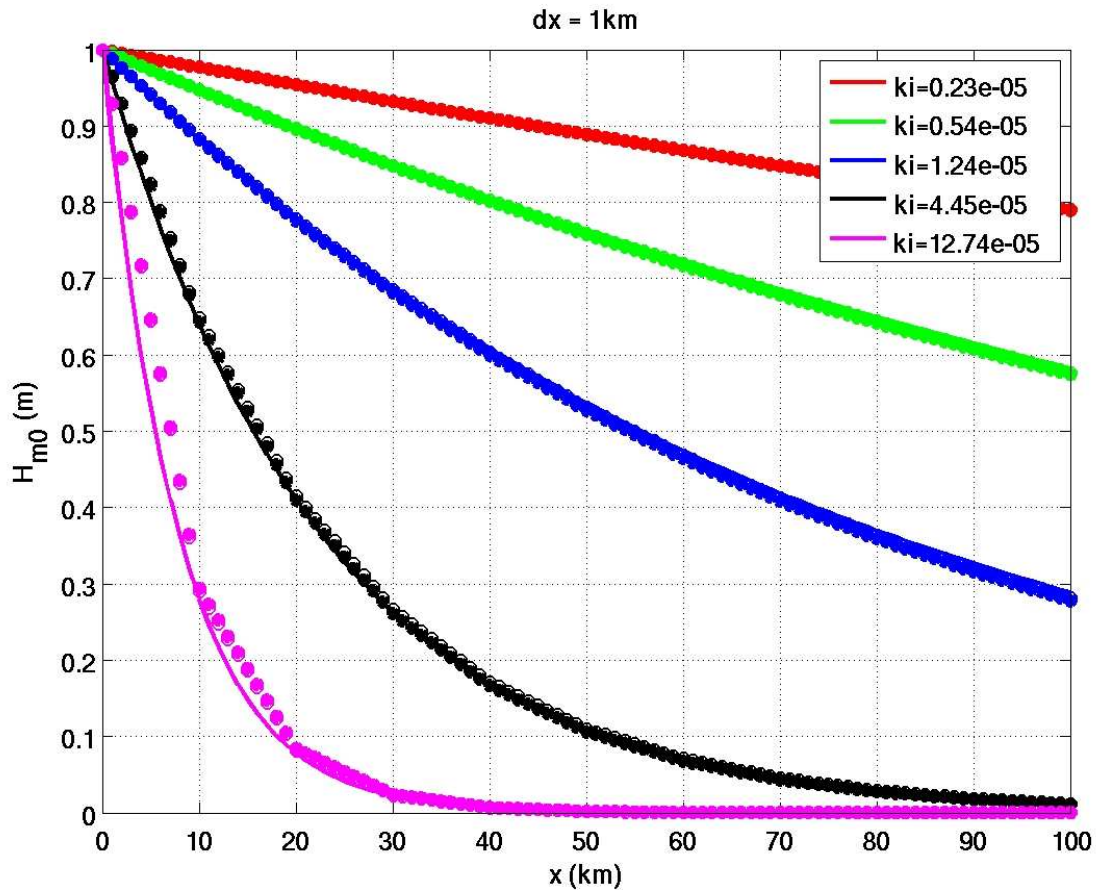
Figure 7. Comparison of WW3-predicted significant wave heights (circles and asterisks) with expected exponential decay (solid lines) for several values of k_i, using grid spacing of Δx = 1 km and mud parameter settings described in the text.

In general, the error levels for the two methods are relatively similar. To limit the maximum error for these simulations to less than 2.7% (to be consistent with Section 3.4), the value of k_i should not exceed roughly 4.5e-05 m^{-1} (for 1-km spacing) or 1.25e-05 m^{-1} (for 5-km spacing).

It is noted that the computational time required by the Dalrymple and Liu (1978) formulation – roughly 30 seconds – is twenty times greater than that required by the Ng (2000) formulation – roughly 1.5 seconds.
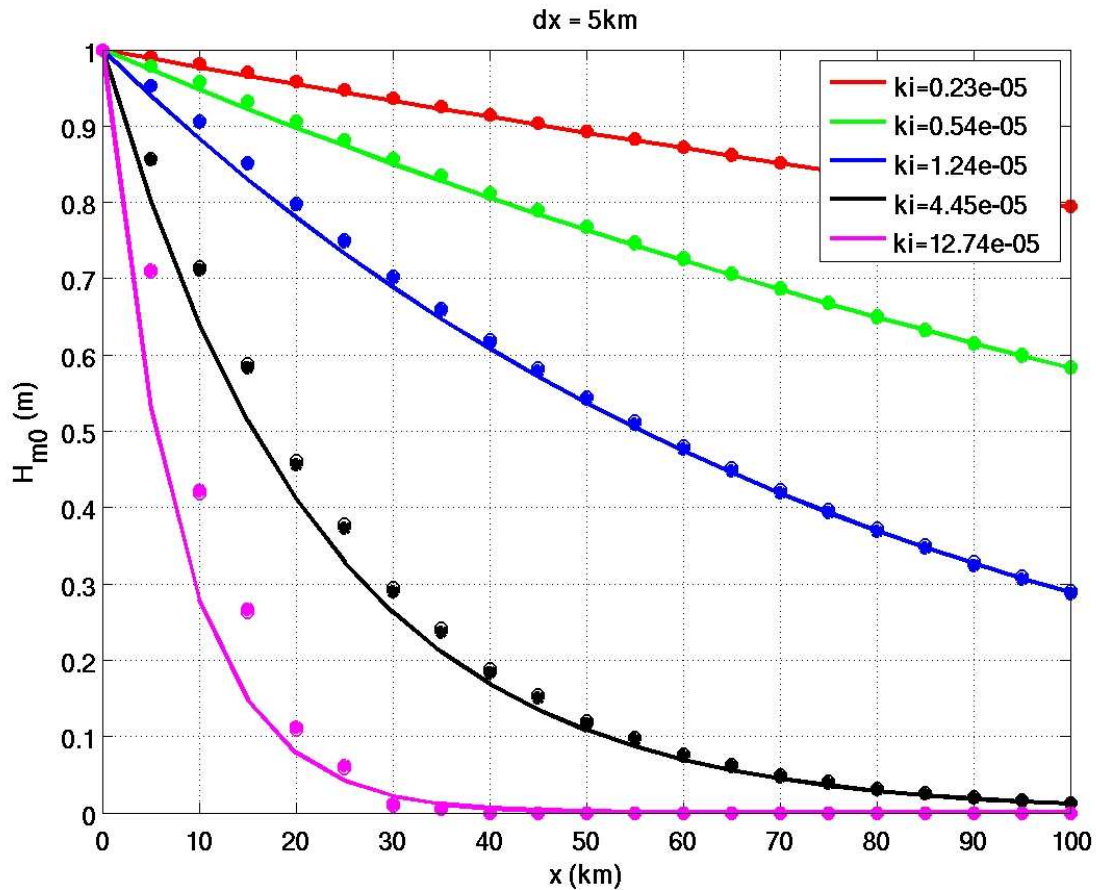
Figure 8. Same as Figure 7, but for Δx = 5km spacing.

4.4   Two-dimensional test case with S_{mud}

This case is similar to the 2d S_{ice} test case. The following is a "bullet list" of features of this test case:

- features that are the same as S_{ice} test:
    - three (3) frequencies from 0.08 to 0.125 Hz
    - nx=101, ny=51
    - Δx=5 km, Δy=10 km
    - boundary forcing from south and east boundaries
    - boundary forcing: θ=135°, f_p=0.10 Hz
    - Starting time : 1968/06/06 00:00:00 UTC
    - Ending time   : 1968/06/07 06:00:00 UTC
- patch of mud in northwest quadrant of domain (x=0 to 25 km, y=25 to 50 km)
- mud density=1310 kg/m^3
- mud thickness=0.4 m
- mud viscosity=7.60E-03 m^2/s

17
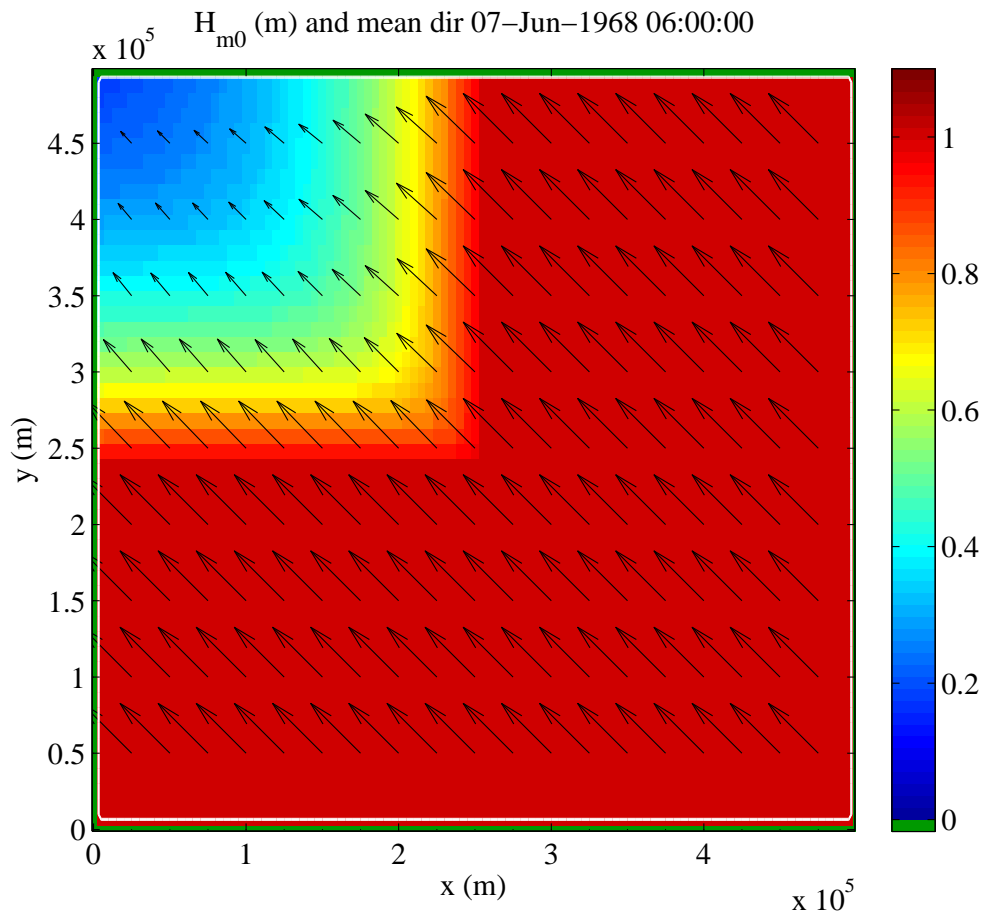
Figure 9. Final state of the two-dimensional test case with S_{mud}, as explained in the text.

The two-dimensional test case displayed a similar difference in required computational time for the two methods to that seen earlier in 1D. For these simulations, the w3sbt8md module based on Dalrymple and Liu (1978) required 9 minutes 39 seconds on a workstation using three cpu cores. In contrast, the w3sbt9md module based on Ng (2000) required only 15.1 seconds. Thus, in this case the Ng (2000) formulation was roughly 38 times faster than that of Dalrymple and Liu (1978).

5   Discussion

Dissemination of code

WW3 has always been an open-source model. During the past several years, the model has started a transition from a code predominantly authored by a single person to a "community model". In fact, in terms of current development, it is unambiguously a community model. The logistics of the collaboration are handled by a Subversion repository at NOAA/NCEP. At present, the code described in this report is not on that svn repository, but is instead on an NRL repository. Our intent is to create a new branch on the NOAA/NCEP repository with this code (and associated test cases) immediately after publication of this report.

Alternate theoretical models for S_{ice}.

From a physical basis, the LHV model is perhaps not the most credible model that can be found in the literature. It was selected as the first model to implement because of its relative simplicity. Other models, for example, require the determination of multiple complex roots, from which one must be selected. A review of other possible methods is given in Section 8. One or more of these will be implemented in WW3 in the future.

Alternatives to calculating S_{ice} within WW3

As we look at more complex theoretical models for S_{ice}, we may find that the computational cost is not practical. In particular, it may be wasteful to make a large number of highly similar yet computationally expensive calculations repeatedly: "highly similar" since in many cases, the ice conditions will be similar in neighboring grid cells, or in consecutive time steps. If the source term is linear, then there is no dependence of $D = S/E$ on spectral energy level, so the spatial and temporal variation of wave conditions becomes irrelevant. Thus, it can be reasoned, that the dissipation rate D might be calculated on a reduced grid, at reduced intervals, and then ingested into WW3 for quick translation onto the computational grid. One paradigm is the "look-up table" approach where WW3 pulls D from a table of pre-calculated values based on many possible ice conditions. Another paradigm is to provide WW3 with 5 to 8 parameters, as $C_{ice,1}(x, y, t)$, $C_{ice,2}(x, y, t)$, ..., $C_{ice,8}(x, y, t)$, also based on some pre-calculations outside of WW3. Then, for a given (x, y, t), the parameters $C_{ice,1}, C_{ice,2}, ..., C_{ice,8}$ (up to 8 numbers) are used to describe the one-dimensional function $D(f)$. [3] The existing method of i/o is more conducive to the second approach.

The simplest approach would be to read in $D(f)$ on a discrete, coarse frequency grid (8 frequencies) and interpolate these numbers onto the model computational grid's n_f frequencies (typically between 25 and 40 frequencies are used). Or, some fitting could be used, e.g. $D(f) = a_0 + a_1 f + a_2 f^2 + a_3 f^3 + a_4 f^4$. In fact, the fitting can be to any parametric form that can be imagined. Matlab is particular powerful in this regard, since it will fit to a user-specified parametric form via least squares.

Finally, we note that WW3 apparently does have the capability to ingest data assimilation data on the computational frequency grid. At time of writing, we are not aware of how mature this piece of code is, but potentially the same methods could be used to ingest $D(f)$ on the model's computational frequency grid.

Future improvement: k_r

As mentioned above, we plan to include the effect of ice and mud on the real part of the wavenumber, k_r, by passing the phase velocity and group velocity variables back to the main routines for calculation of refraction and shoaling effects.

Unresolved complication: other source terms in presence of ice

It stands to reason that the deepwater source terms S_{in}, S_{ds} and S_{nl4} do not behave the same under partial ice cover as they do in open water. The most simple way to address this would be to multiply each term by the open water fraction, $(1 - \epsilon)$. This will be our initial approach[4].

---

[3] Keep in mind that $D(f)$, $k_i(f)$ and $\alpha(f)$ are all dissipation rates and are directly related, so if one is known, the others are known.

[4] A time of writing, this is not done yet, though apparently the ST4 source term package already reduces S_{in} in this manner. Ideally, this operation should be performed at a higher level than the individual source term packages, to ensure uniformity.

However, this simple approach is not necessarily the best: this warrants further consideration and study. Observational data and more process-based modeling might help with this question.

Applicability of S_{mud} within a conditionally stable model
WW3, run on structured grids (either regular or irregular types), is conditionally stable. As such, there is a practical limit on how fine the geographic resolution can be set. Often, this will discourage applications in the littoral, such as the application of SWAN by Rogers and Holland (2009), where $\Delta x = 252$ m (two-dimensional case) and $\Delta x = 50$ m (one-dimensional case), where the unconditionally stable—and optionally stationary—SWAN must be considered as a more efficient alternative to WW3. This, in turn, makes physical representation of wave-seafloor interaction a lower priority in WW3 than in SWAN. Even so, these interactions can be significant on broad continental shelves modeled at resolutions more appropriate to WW3, e.g. $\Delta x = 4$ km; a specific example would be the North Carolina shelf, which is O(80 km) across, e.g. see Ardhuin et al. (2003). Further, methods are being introduced to enable higher resolution applications of WW3. Van der Westhuysen and Tolman (2012) introduced a quasi-stationary method of computation that can be regarded as a compromise (or hybrid) between the stationary mode of computation optionally used with SWAN and traditional time-stepping, which was the only method available in WW3 prior. Further, the unstructured-grid methods of Roland et al. (2009) have been implemented in an experimental version of WW3. Both developments suggest that, in the near future, it will be possible to make computationally efficient applications of WW3 at high resolution.

Closing remarks
On the subject of the S_{ice} implementation in WW3, and the question "why was this not done sooner?", as noted earlier, the argument has been that the treatment of ice as a partial blocking mechanism via ice concentration (Tolman 2003) is sensible, as: a) ice concentration is the only operationally available ice variable, b) the method is relatively cheap, and c) the end result is very similar to what the more sophisticated S_{ice} might provide. We accept (a) and (b) as legitimate arguments, but (c) is doubtful, since the original method is dependent on grid resolution and aspect ratio, requiring grid-specific recalibration. Even (c) becomes a reasonable argument if one considers the recent improvements to this part of the code by Ifremer (see Section 3.2). In this regard, the S_{ice} implementation herein might be regarded as somewhat in advance of what would be feasible operationally. This is a traditional problem with wave modeling: features become available which will not always be applicable due to limits on input. For example, a high-resolution two-dimensional littoral wave model will not generally have adequate bathymetry in an operational context; this is the traditional argument for using simple one-dimensional "surf models" operationally. Similar statements could be made regarding the availability of mud thickness, viscosity, and density. These are valid arguments, but two counter-arguments can be made. First, we can anticipate that as technology external to the wave model improves, more information about the ice will become available. For example, ice thickness or floe size distribution might be derived from ice model or remote sensing in the near future; NRL is now actively researching methods to derive ice thickness from satellite. Second, these new routines can be applied in non-operational contexts, where the ice (or mud) is more adequately prescribed, such as the case with hindcasts corresponding to field experiments, already planned with newly funded Office of Naval Research initiatives. Lastly, we point out that the simpler methods, even after the Ifremer updates, do not provide for dependence of attenuation on wave frequency or the dependence of phase velocity and group velocity on ice. Though the

quantitative dependencies still need to be worked out, the existence of such dependencies is clear enough and should be accommodated in subsequent research codes.

6   References

Ardhuin, F., W.C. O'Reilly, T.H.C. Herbers, and P.F. Jessen, 2003: Swell transformation across the continental shelf. Part I: Attenuation and directional broadening. *J. Phys. Oceanogr.*, **33**, 1921-1939.

Booij, N., R.C. Ris, and L.H. Holthuijsen, 1999: A third-generation wave model for coastal regions, Part 1: Model description and validation. *J. Geophys. Res.* **104** (C4), 7649-7666.

Brennecke, B., 1921: Die ozeanographischen Arbeiten der Deutschen Antarktischen Expedition 1911-1912, *Arch. Dtsch. Seewarte*, **39** (206).

Dalrymple, R.A., and P.L.F. Liu, 1978: Waves over soft muds: a two-layer fluid model. *J. Phys. Oceanogr.*, **8**, 1121-1131.

De Wit, P.J., 1995. Liquefaction of cohesive sediment by waves. PhD dissertation. Delft University of Technology, the Netherlands.

Dumont, D., A. Kohout, and L. Bertino, 2011: A wave-based model for the marginal ice zone including a floe breaking parameterization, *J. Geophys. Res.*, **116**, C04001, doi:10.1029/2010JC006682.

Gade, H.G., 1958: Effects of a non-rigid, impermeable bottom on plane surface waves in shallow water. *Journal of Marine Research* **156** (2), 61-82.

Hodur, R. M., 1997: The Naval Research Laboratory's Coupled Ocean/Atmospheric Mesoscale Prediction System (COAMPS). *Mon. Wea. Rev.*, **125**, 1414-1430.

Hunkins, K., 1966: Ekman drift current in the Arctic Ocean, *Deep Sea Res.*, **13**, 607-620.

Jiang, L. and Mehta, A.J., 1996. Mudbanks of the southwest coast of India. V: Wave attenuation. *J. Coastal Res.* **12**(4), 890-897.

Keller, J.B., 1998: Gravity waves on ice-covered water. *J. Geophy. Res.*, **103** (C4): 7663-7669.

Kohout, A.L. and M. H. Meylan, 2008: An elastic plate model for wave attenuation and ice floe breaking in the marginal ice zone, *J. Geophy. Res.*, **113**, C09016, doi:10.1029/2007JC004434.

Komen, G. J., Cavaleri, L., Donelan, M., Hasselmann, K., Hasselmann, S., and P.A.E.M. Janssen, 1994: *Dynamics and Modelling of Ocean Waves.* Cambridge Univ. Press, 532 pp.

MacPherson, H., 1980:The attenuation of water waves over a non-rigid bed. *J. Fluid Mech.* **97**(4), 721-742.

Masson, D. and P. H. LeBlond, 1989: Spectral evolution of wind-generated surface gravity waves in a dispersed ice field, *J. Fluid Mech.*, **202**, 43-81.

Mei, C.C. and Liu, K.-F., 1987: A Bingham-plastic model for a muddy seabed under long waves. *J. Geophys. Res.* **92**, 14581-14594.

Newyear, K. and S. Martin, 1999: Comparison of laboratory data with a viscous two-layer model of wave propagation in grease ice, *J. of Geophys. Res.*, **104** (C4), 7837-7840.

Ng, C.O., 2000: Water waves over a muddy bed: a two-layer Stokes' boundary layer model. *Coastal Engineering*, **40** (3), 221-242.

Liu, A.K. and E. Mollo-Christensen, 1988: Wave propagation in a solid ice pack. *J. Phys. Oceanogr.*, **18**, 1702-1712.

Liu, A.K., B. Holt, and P.W. Vachon, 1991: Wave propagation in the Marginal Ice Zone: Model predictions and comparisons with buoy and Synthetic Aperture Radar data. *J. Geophys. Res.*, **96**, (C3), 4605-4621.

Liu, A. K., S. Hakkinen, and C. Y. Peng, 1993: Wave effects on ocean-ice interaction in the marginal ice zone, *J. Geophy. Res.*, **98** (C6), 10025-10036.

Perrie, W. and Y. Hu, 1996: Air-ice-ocean momentum exchange. Part I: Energy transfer between waves and ice floes, *J. Phys. Oceanogr.*, **26**, 1705-1720.

Posey, P. G., E. J. Metzger, A. J. Wallcraft, R. H. Preller, O. M. Smedstad, and M.W. Phelps, 2010: "Validation of the 1/12° Arctic Cap Nowcast/Forecast System (ACNFS). *Naval Research Laboratory Memorandum Report NRL/MR/7320-9287.*

Rogers, W. E., and T. J. Campbell, 2009: Implementation of Curvilinear Coordinate System in the WAVEWATCH-III Model. *NRL Memorandum Report: NRL/MR/7320-09-9193*, 42 pp.

Rogers, W.E., and K.T. Holland, 2009: A study of dissipation of wind-waves by mud at Cassino Beach, Brazil: prediction and inversion. *Continental Shelf Research*, **29**, 676-690.

Roland, A., A. Cucco, C. Ferrarin, T.-W. Hsu, J.-M. Liau, S.-H. Ou, G. Umgiesser, and U. Zanke, 2009: On the development and verification of a 2-D coupled wave-current model on unstructured meshes, *J. Mar. Syst.*, **78**, S244–S254.

Sepp, M. and J. Jaagus, 2011: Changes in the activity and tracks of Arctic cyclones. *Climatic Change*, **105**, 577-595.

Squire, V. A., 1984: A theoretical, laboratory, and field study of ice-coupled waves, *J. Geophy. Res.*, **89** (C5), 8069-8079.

Squire, V. A., 2007: Of ocean waves and sea-ice revisited, *Cold Regions Science and Technology*, **49**, 110–133.

Squire, V. A., J. P. Dugan, P. Wadhams, P. J. Rottier, and A. K. Liu, 1995: Of ocean waves and sea ice, *Annu. Rev. Fluid Mech.*, **27**, 115-168.

Squire, V. A., G. L. Vahghan, and L. G. Bennetts, 2009: Ocean surface wave evolvement in the Arctic Basin, *Geophys. Res. Lett.*, **36**, L22502, doi:10.1029/2009GL040676.

Tolman, H.L., 1991: A Third generation model for wind-waves on slowly varying, unsteady, and inhomogeneous depths and currents. *J. Phys. Oceanogr.* **21(6)**, 782-797.

Tolman, H. L. 2003: Treatment of unresolved islands and ice in wind wave models. *Ocean Modelling*, **5**, 219-231.

Tolman, H.L. 2008: A mosaic approach to wind wave modeling. *Ocean Modelling*, **25**, 35-47.

Tolman, H.L., 2009: User Manual and System Documentation of WAVEWATCH III™ Version 3.14, Tech. Note, NOAA/NWS/NCEP/MMAB, 220 pp.

Tolman, H.L., B. Balasubramaniyan, L.D. Burroughs, D.V. Chalikov, Y.Y. Chao, H.S. Chen, and V.M. Gerald, 2002: Development and implementation of wind-generated ocean surface wave models at NCEP. *Weather and Forecasting (NCEP Notes)*, **17**, 311-333.

van der Westhuysen, A.J. and H.L. Tolman, 2012: Quasi-stationary WAVEWATCH III® for the nearshore, 12*th* *International Workshop on Wave Hindcasting and Forecasting*, 16 pp.

Vaughan, G. L., L. G. Bennetts, and V. A. Squire, 2009: The decay of flexural-gravity waves in long sea ice transects, *Proc. R. Soc. A*, **465**, 2785-2812, doi: 10.1098/rspa.2009.0187.

WAMDI Group, 1988: The WAM model--A third generation ocean wave prediction model. *J. Phys. Oceanogr.,* **18***,* 1775-1810.

Wadhams, P., 1973a: *The effect of a sea ice cover on ocean surface waves*. PhD thesis. Univ. Cambridge, UK, 223 pp.

Wadhams, P., 1973b: Attenuation of swell by sea ice, *J. Geophys. Res.* **78**, 3552-3563.

Wadhams, P. and B. Holt, 1991: Waves in frazil and pancake ice and their detection on Seasat SAR imagery. *J. of Geophys. Res.*, **96** (C5), 8835-52.

Wadhams, P., V. A. Squire, J. A. Ewing, R. W. Pascal, 1986: The effect of marginal ice zone on the directional wave spectrum of the ocean. *J. Phys. Oceanogr.*, **16**, 358-76.

Wadhams, P., V. A. Squire, D. J. Goodman, A. M. Cowan, and S. C. Moore, 1988: The attenuation rates of ocean waves in the marginal ice zone, *Journal of Geophysical Research*, **93**, 6799–6818.

Wang, R. and H. H. Shen, 2010: Gravity waves propagating into ice-covered ocean: a visco-elastic model. *J. Geophys. Res.* 115, C06024, doi:10.1029/2009JC005591.

Weber, J. E. 1987: Wave attenuation and wave drift in the marginal ice zone. *J. Phys. Oceanogr.*, **17**, 2351-61.

Winterwerp, J.C., de Graaff, R.F., Groeneweg, J., Luyendijk, A.P., 2007: Modelling of wave damping at Guyana mud coast. *Coastal Eng.*, **54**: 249-261.

Zhang, X.-Y. and Ng, C.-O., 2006: Mud-wave interaction: a viscoelastic model. *China Ocean Eng.*, **20**(1), 15-26.

7 Further Reading

Broström, G. and K. Christensen, 2008: Waves in sea ice, *Norwegian Meteorological Institute Report*, No. 5.

Hasselmann, K., 1966: Feynman diagrams and interaction rules of wave-wave scattering processes, *Rev. Geophys.*, **4**(1), 1–32, doi:10.1029/RG004i001p00001.

Hunkins, K., 1962: Waves on the Arctic Ocean, *J. Geophy. Res.*, **67**(6), 2477-2489.

Hwang, P. A., D. W. Wang, E. J. Walsh, W. B. Krabill, and R. N. Swift, 2000: Airborne measurements of the wavenumber spectra of ocean surface waves. Part 1. Spectral slope and dimensionless spectral coefficient. *J. Phys. Oceanogr.,* **30**, 2753-2767.

Kwok, R., G. F. Cunningham, M. Wensnahan, I. Rigor, H. J. Zwally, and D. Yi, 2009: Thinning and volume loss of the Arctic Ocean sea ice cover: 2003–2008, *Journal of Geophysical Research*, **114**, C07005, doi:10.1029/2009JC005312

Liu, A. K., P. W. Vachon, C. Y. Peng, and A. S. Bhogal, 1991: Wave attenuation in the marginal ice zone during LIMEX, *Atmosphere-Ocean*, **30**, 192-206.

Liu, A. K., C. Y. Peng and T. J. Weingartner, 1994: Ocean-ice interaction in the marginal ice zone using synthetic aperture radar imagery*, Journal of Geophysical Research*, **98**, 22391-22400.

Lu, P., Z. J. Li, Z. H. Zhang, and X. L. Dong, 2008: Aerial observations of floe size distribution in the marginal ice zone of summer Prydz Bay, *Journal of Geophysical Research,* **113**, C02011, doi:10.1029/2006JC003965.

Schulz-Stellenfleth, J. and S. Lehner, 2002: Spaceborne synthetic aperture radar observations of ocean waves travelling into sea ice, *Journal of Geophysical Research*, **107**, C8, 10,1029-10,1039.

Vachon, P. W., R. B. Olsen , G. E. Livingstone, and N. G. Freeman, 1988: Airborne SAR imagery of ocean surface waves obtained during LEWEX: Some initial results, *IEEE Transactions on Geoscience and Remote Sensing*, 26, 548-561.

8 Appendix: Brief review of literature regarding S_{ice} calculation methods

There is no shortage of theoretical models for representing the effects of waves on ice. The larger challenges are to select the most appropriate models, to apply them only in applications consistent with their underlying assumptions, and to determine the most suitable inputs for these models, since they unfortunately are universally *not* framed in terms of variables that are available operationally. We give a brief, partial survey of available models here. Though we are

primarily interested in the MIZ, models for the continuous ice problem are discussed here. A more detailed review can be found in Squire et al. (1995), since updated by Squire (2007).

There are a few broad categories of models for the MIZ. The first that we will discuss is the type of model based on scattering from individual floes. Squire et al. (1995) argue quite reasonably that this type of model is most appropriately used in situations of less compact ice. This method is given by Wadhams (1973a) and described in Wadhams et al. (1986, 1988). This model requires a distribution of floe diameter d_i and thickness h_i. Masson and LeBlond (1989) also derive a "scattering by floes" model assuming cylindrical floes (circular from top view) organized in a hexagonal pattern. It requires floe draft, radius, water depth, and distance to other floes. Perrie and Hu (1996) based their model on this one. Kohout and Meylan (2008) have a similar model, requiring the mean size of floes, and ice concentration. Dumont et al. (2011) use this model.

The second type is more appropriately used in situations where the ice floes are more compact, potentially colliding. Here, the floes are treated as a single layer with specific rheology[5]. Weber (1987) and Keller (1998) treat this ice cover as a viscous fluid layer in models for broken ice (frazil, brash, pancake); they require effective viscosity (or eddy viscosity) and density. Newyear and Martin (1999) use this model in a study of grease ice. The Wang and Shen (2010) "unified rheological model" is similar to Keller (1998) but adds elasticity; elasticity must be quantified via the effective shear modulus G. A particular challenge in this type of model is to recreate the so-called "roll-over" of dissipation seen in many observations, which is technical jargon for the non-monotonic dependence of the dissipation rate on wave period.

The third type of model is similar to the second, insofar as it is intended for highly compact ice (e.g. shore-fast ice), but instead of presenting the problem in terms of two "fluid" layers with the dissipation being caused by the rheology of the ice layer, here the dissipation is attributed to "eddy viscosity in the turbulent boundary layer beneath the ice". An example of this model is Liu and Mollo-Christensen (1988) which is used by Liu et al. (1991) and Liu et al. (1993) in combination with a model for continuous ice, Wadhams (1973b).

The fourth type of model for the MIZ is described by Squire et al. (1995) as a "mass-loading model". The Wadhams and Holt (1991) model is one example. This type of model is of less interest to the present study, since it does not predict attenuation, i.e. dissipation rate $k_i = 0$ (see Section 1). However, the propagation velocity is affected via modification of the real part of the wavenumber k_r, so it can block slower waves in a manner similar to blocking of short wind waves by opposing currents.

The continuous ice models are most often associated with wave propagation through the central Arctic, though there is applicability to shore-fast ice and perhaps highly compact sea ice. Wadhams (1973b) presents one such model, based on plastic-elastic deformation of the ice sheet by swell; plastic deformation or "creep" provides the actual dissipation. This is applied by Liu et al. (1991) and Liu et al. (1993) to the MIZ problem along with the boundary layer model as mentioned above. Here solution for k requires E (Young's modulus of elasticity), B (coefficient

---

[5] We acknowledge the apparent contradiction of treating discontinuous ice as a continuous layer. Since the situation being modeled is not continuous, we prefer not to group this under the category of "continuous ice model".

for bending) and *M* (coefficient for inertia of the ice). Squire (1984) also presents a model for "shore-fast ice"; here, there is a linear viscoelastic plate over a fluid; the viscous quality is intended to represent creep in the ice layer.

A second broad category of continuous ice model is that used by Vaughan et al. (2009) and Squire et al. (2009). This model is based on scattering from discontinuities in ice thickness, thus requiring ice thickness profile along axis of wave propagation. Squire et al. (2009) use this model to predict dissipation rates using ice thickness profiles from upward-looking sonar collected by a submarine.